Hindawi
Advances in Polymer Technology
Volume 2022, Article ID 8988568, 16 pages
https://doi.org/10.1155/2022/8988568

Research Article

Investigating the Effects of Nonsolvent Additive and Spinning Conditions on Morphology and Permeation of PAN Hollow Fiber Membranes

Mohammad Ali Ghadiri, Ahmad Beyranvand, and Sheida Morsali

Membrane Science and Technology Research Group, Department of Chemical Engineering Tarbiat Modares University, Tehran, Iran

Correspondence should be addressed to Mohammad Ali Ghadiri; ghadiri.ma@modares.ac.ir

Received 11 February 2022; Revised 27 March 2022; Accepted 30 March 2022; Published 22 April 2022

Academic Editor: Gyorgy Szekely

In this study, polyacrylonitrile hollow fiber (PAN HF) membranes were designed and fabricated with desired morphology and permeability for low pressure-driven applications via the dry-wet phase-inversion spinning process. The effects of multiple design and fabrication parameters on permeation, morphology, thickness, and pore size of membranes were investigated using various techniques. Moreover, the effects of water as the nonsolvent additive, chemical composition of the bore solution, dope solution flow rate, air gap, coagulation bath temperature, and tensile ratio (take-up speed) were investigated. The addition of 3% wt. water as the nonsolvent additive into the dope solution resulted in a seventeen-times increment in the water flux up to 495 $L\,m^{-2}\,h^{-1}\,bar^{-1}$. It showed a significant improvement in membrane porosity compared with those prepared without water nonsolvent additive. Utilization of 90% wt. of the solvent in water solution as the bore solution instead of pure water showed the most significant effect on the water flux and membrane structure among the fabrication parameters. It resulted in a reduction in threshold permeation pressure by more than ten times. The results revealed that whichever variation, including increased dope solution flow rate or coagulation bath temperature, or reduced air gap or traction, leads to promotion of membrane water flux. Still, different effects on the structure and morphology of the membranes were observed. Based on the outcomes of this study and according to the SEM images, one can conclude that outer surface pore size reduction from about 300 nm resulted in decreased water flux from 448 to 226 $L\,m^{-2}\,h^{-1}\,bar^{-1}$, so that no pores were observed in the outer surface until 50 K magnification of the SEM image. The findings in this study provide instructive guidelines for the design and fabrication of high-performance hydrophilic PAN-based hollow fiber membranes with the desired morphology and water flux. Best ranges of investigated parameters for relatively high permeate water flux and desired membrane morphology were reported.

1. Introduction

Nowadays, many people do not have access to potable water, posing serious health problems caused by different pollutants, especially pathogenic microorganisms [1]. Older water preparation methods such as dam construction and digging wells permanently failed to solve this problem. They made the situation more complicated due to environmental damage that they could inflict [2]. As a result, novel water purification methods such as portable water devices can play an essential role in this case.

Various technologies can be used for water purification, such as distillation, solar purification, and membrane separation. Many factors are considered to choose the optimal method for this purpose, including efficiency, simplicity, convenience, equipment, affordability, and environmental issues [3]. Membranes are of high interest among all the water purification methods due to their desirable characteristics. Easy operation, ability to remove turbidity and various types of microbial contaminants, energy-saving, and economic profits are advantages of membrane application to produce potable water.

Table 1: State of the art for PAN hollow fiber membrane.

Dope chemical composition	Application	Investigated parameters	Reference
PAN/DMF: 15/85	Ultrafiltration	Solvent amount in coagulation bath, draw ratio (take-up speed)	[34]
PAN/DMF/PEG: 22/78/0-30	Pervaporation	Posttreatment with a water bath, a dry air oven heat-treatment, PEG content, PEG molecular weight	[35]
PAN/DMF: 22/78	Pervaporation	Heat-treatment temperature, feed composition, feed solution temperature	[36]
PAN/PVP/$ZnCl_2$/DMF: 15-20/0-0.5/0-3/80-82	Ultrafiltration	Flow rate of polymer dope, bore liquid, polymer concentration, speed of polymer pump, feed pressure	[37]
Self-made PAN HFMs membranes)MWCO 60000 Da)	Packing in distillation	Heat treatment time and temperature, thermal and chemical stability in solvents	[38]
PAN/$CaCl_2$/DMF: 18/1/81	Ultrafiltration	PAN/LiCl and PAN/$CaCl_2$ ratios	[39]
PAN/PVP1100-1400 kDa/NMP: 8-12/2-6/86	Ultrafiltration	Virus filtration, fouling	[40]
Purchased PAN HFM (MWCO: 60 000 Da)	Gas separation	Chemical modification provided by a covalent linker between the MOF layer and PAN substrate, chemical and mechanical stability	[41]
PAN/PVP K30/DMSO: 17.0/4.0/79.0	Ultrafiltration	Dope composition, bore fluid, dope flow rate, bore fluid flow rate, take-up speed	[42]
PAN/PVP 360 K/DMF/propane diol: 18/78/3/1	Ultrafiltration	Air gap, modification with hypochlorite	[43]

Low-pressure membranes, especially ultrafiltration membranes (UF), can eliminate aquatic pathogens, microorganisms, and colloidal substances due to their pore size range (between 10 and 100 nm) to provide safe drinking water. Water purification with ultrafiltration membranes is a simple process without adding any disinfectants or chemicals [2]. Hollow fiber membrane modules are prevalent among different membrane modules for potable water production due to their advantages: large surface area per volume, low cost per unit area, mechanical stability, back-flush ability, and good flexibility.

Hollow fiber membranes for drinking water production can be fabricated using diverse membrane materials. Polyacrylonitrile (PAN), with polar nature, is one of the materials that can form hollow fibers due to its hydrophilicity, mechanical, and thermal stability (more than 120, and resistance to most solvents, chemicals, bacteria, and radiation). Due to the high hydrophilicity of polyacrylonitrile compared to other common polymers such as polyvinylidene fluoride, polyethylene, and polysulfone, they are less liable to be fouled in aquatic environments. Polyacrylonitrile is also commercially available and has a reasonable price. Due to the polar nitrile groups in the PAN structure can be easily modified by chemical methods [4]. An extensive series of studies have been carried out to investigate the effect of different design and fabrication parameters and modification techniques on spinning PAN hollow fiber ultrafiltration membranes. Although improvements have been made in the fabrication of PAN hollow fibers, more studies on this matter under various spinning conditions are required to understand better the formation mechanism of membranes and the correlation between membrane morphology and permeation performance UF processes.

PAN hollow fiber membranes with desirable asymmetric structures can be prepared via a nonsolvent induced phase separation process. Ease of processing and facile modulation are the main reasons for the broad application of this fabrication technique [5–7]. Although the phase separation method is a simple method for membrane fabrication, the final properties of the membrane are highly dependent on several factors such as polymer concentration, solvent type, dope polymer viscosity, coagulation bath composition, temperature, chemical nature, the concentration of additive, room relative humidity, bore fluid type, spinneret design, dope and bore flowrate, air gap distance, and the stretch ratio [5, 7, 8]. Combining the mentioned factors complicates the path to achieving the desired morphology. A literature overview demonstrates different and contradictory results in diverse polymeric systems.

Moreover, to enhance PAN hollow fiber membranes' performance, selectivity, and other characteristics, they should be modified through different methods. Using additives in the polymer solution is a dominant procedure to manipulate membrane structure to promote pore formation, pore interconnectivity, polymer solution viscosity, and change in mutual affinity between polymer solution components. Polymer solution additives can be classified into nonsolvent additives, such as water, alcohols, and acetone [9–13]; and polymeric additives, such as polyethylene glycols (PEG), polyvinylpyrrolidone (PVP), and pluronic copolymers [14–17]; and salt or inorganic additives such as LiCl, TiO2, and H3PO4 [18–20]. Among the above classification, nonsolvent additives such as water have a more noticeable influence on membrane morphology than others. Also, it is shown that the concentration and molecular weight of polymeric additives, especially PVP as a porosity-causing agent, directly affect kinetic hindrance and hydraulic resistance of hollow fiber membranes [20]. Table 1 summarizes the state of the art for PAN-based hollow fiber membranes, and as can be seen, little attention and lack of experimental research

to use various spinning conditions. So more study on the preparation of PAN-based hollow fiber membranes under different spinning conditions is needed to understand their formation mechanism better.

In the present work, PAN hollow fiber membranes were fabricated via the dry/wet-spinning process to study the effect of water concentration as a nonsolvent additive in the dope solution and different spinning conditions. Their structure was characterized by scanning electron microscopy (SEM), pure water flux, porosity, and mean pore size. The objective was to prepare PAN hollow fibers with different pore sizes for microfiltration and low-pressure ultrafiltration applications. This study is intended to prepare PAN microporous hollow fiber membranes with desired pore structure and performance in water purification.

2. Experimental

2.1. Materials. Polyacrylonitrile (PAN, molecular weight (MW): 90000 g. mol^{-1}, density: 1.184 g. cm^{-3}) in powder form was supplied by Polyacryl Co., Isfahan, Iran, and employed as the main polymer for dope solution preparation. N-Methyl-2-pyrrolidone (NMP, industrial grade, boiling point: 202°C, density: 1.04 g. cm^{-3}) from Medichem Enterprise Company (China) was used as the solvent to prepare dope and bore solutions and rinse spinneret mainly because of its high solubility, less dangerous, and more available. Polyvinylpyrrolidone K30 (PVP, molecular weight (MW): 40000 g. mol^{-1}, density 1.2 g. cm^{-3}) from Rahavard Tamin Company (Iran) was employed as an additive in the dope solution to make pores in the membrane structure and improve hydrophilicity. Deionized water (molecular weight (MW): 18.01528 g. mol^{-1}, density: 0.997 g. cm^{-3}) was used as a part of the bore solution, nonsolvent additive in dope solution, and the remaining solvent exchange process in the membranes after spinning. Tap water was employed as the external coagulation bath.

2.2. Fabrication of Outer Selective PAN Hollow Fiber Membranes

2.2.1. Dope Solution Preparation. Dope solution for the spinning process was prepared by dissolving the specified amount of polymer and pore former additive into a mixture of solvent and nonsolvent additive that was first weighed according to the final volume. PVP and water were used as the pore former and nonsolvent additive to the dope solution, respectively. Different dope solutions with various PAN/NMP/water/PVP compositions were similarly prepared as comparisons. The total concentration of PAN/solution was kept constant at 18%. PVP and PAN powder were gradually poured into the mixture of solvent and nonsolvent in a double-openings flat bottomed balloon half-placed into a water container on a heater stirrer adjusted at 70°C (the desired result PAN dissolution temperature in the NMP). A mechanical stirrer continuously homogenized the dope solution until the polymer was completely dissolved. One of the balloon openings was closed with a cork, while the other was opened to prevent the escape components from evaporating. The homogeneous dope prepared was cooled down to the room and degassed overnight before spinning. The polymeric hollow fiber membrane spinning semi-industrial pilot process flow diagram by the dry-wet phase separation method used in this study is shown schematically in Figure 1. The dope solution was poured into the cylinder of the syringe pump of the spinning equipment and fed into the transparent polypropylene hose, held in the same way for almost a night at room temperature to ensure degassing and subsequently air bubbles eliminating before the spinning process. The more the viscosity of the solution increases, the longer it takes the solution to be degassed.

2.2.2. Spinning of PAN Hollow Fiber Membranes. The degassed homogeneous dope solution was used to fabricate PAN hollow fiber membranes with the dry-jet wet phase inversion method through the spinning process. The bore fluid was varied from water to a mixture of NMP/water. The spinning equipment's command-and-control panel formulated dope and bore solution flow rates, and the collection speed at the take-up drum was set. After passing through a filter with a diameter of about 10 micrometers, the spinning dope and bore solutions were, respectively, delivered to the outer and inner tube of the spinneret by syringe pumps then were entered into the spinneret. When the spinning dope and the bore solutions met at the tip of the spinneret, they were immersed into the coagulation bath containing tap water after leaving the spinneret and passing the adjusted air gap between the spinneret and the water bath. When the membrane reaches the end of the coagulation bath, the phase inversion is completed, and the nascent membrane forms hollow fibers. Then, by directing the fibers to the middle rollers, the fibers were first entered into the tap water washing tank and then into the take-up drum. During the rotation of the take-up drum and the hollow fibers winding on it, the fibers were kept wet by pumping water by a small pump. Finally, after the spinning process and solidification, the various samples were removed from the take-up drum and separated. The as-spun fibers were immersed in a deionized water bath at room temperature for two days to remove residual solvent before further study. Then, they were immersed in 50% glycerin solution for two days. The surface tension between glycerin solution and polyacrylonitrile is less than the surface tension between water and this polymer, which prevents the membrane structure from being destroyed due to the capillary force applied to the polymer during the solvent exchange process. Finally, the hollow fiber membranes were hung in the ambient air for a day to complete drying and solvent evaporation before module fabrication. The polymer dope and bore fluid compositions and spinning parameters are listed in Table 2.

2.3. Characterization of the Membranes

2.3.1. SEM Analysis. The fabricated PAN hollow fiber membranes' surface and cross-sectional morphologies and pore structure were characterized using scanning electron microscopy (FEI ESEM, QUANTA 200, USA). Imaging prepared samples according to the type of imaging test by BSE and

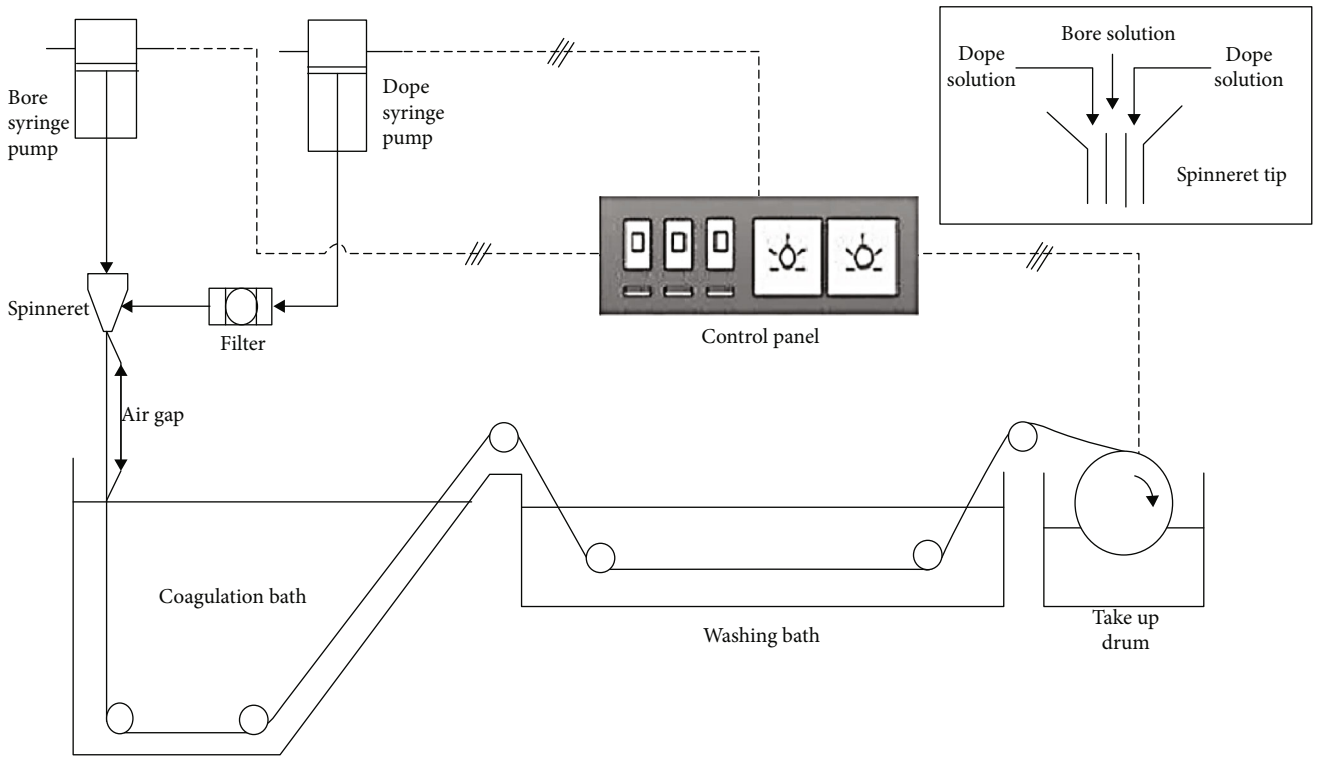

Figure 1: The process flow diagram of the spinning device used in this study.

Table 2: Composition and the spinning conditions of the fabricated hollow fiber PAN membranes. Spinneret OD/ID (mm), 1.2/0.6; polymer concentration, 18 wt%; PVP concentration, 4 wt% of total polymer solution weight; dope/bore flow rate, 1.5; coagulant, tap water.

No.	Membrane code	Dope composition NMP/H2O (wt%/wt%)	Bore fluid composition NMP/H_2O (*v*/*v*, %)	Dope flow rate (ml)	Air gap distance (cm)	Coagulation bath temperature	Take-up status
1	W0	82/0	90/10	6	2	28	Free fall
2	W2	80/2	90/10	6	2	28	Free fall
3	W3.5	78.5/3.5	90/10	6	2	28	Free fall
4	W6	76/6	90/10	6	2	28	Free fall
5	B0	82/0	0/100	4	2	28	Free fall
6	B90	82/0	90/10	4	2	28	Free fall
7	D4	78.5/3.5	90/10	4	2	28	Free fall
8	D6	78.5/3.5	90/10	6	2	28	Free fall
9	A5	78.5/3.5	90/10	6	5	28	Free fall
10	A7	78.5/3.5	90/10	6	7	28	Free fall
11	A9	78.5/3.5	90/10	6	9	28	Free fall
12	C22	78.5/3.5	90/10	6	5	22	Free fall
13	C28	78.5/3.5	90/10	6	5	28	Free fall
14	T0	78.5/3.5	90/10	6	2	28	Free fall
15	T10	78.5/3.5	90/10	6	2	28	10% stretch
16	T20	78.5/3.5	90/10	6	2	28	20% stretch

SE detectors in various magnifications were conducted. Images were taken from the cross-section and the outer surface of the fabricated hollow fibers. The dried hollow fiber membranes were fractured in liquid nitrogen so that samples exposed their cross-sectional morphology. Before the analysis, samples were treated for sputter-coating by a PVD device (COXEM, South Korea). The ImageJ software was used for pore size, outer and inner diameters, and membrane thickness measurements in the images.

2.3.2. Pure Water Flux Measurement. The pure water flux experiments of the prepared membranes were analyzed

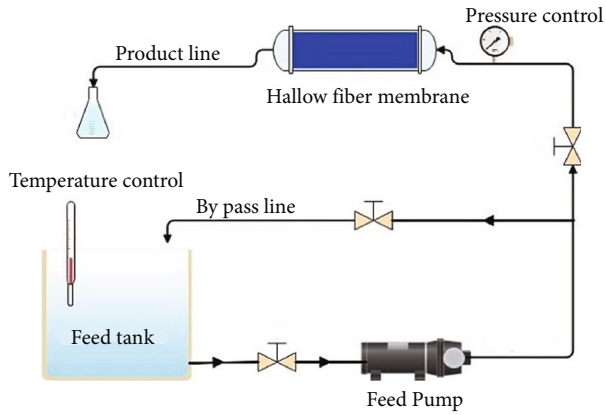

Figure 2: Schematic diagram of water separation system setup.

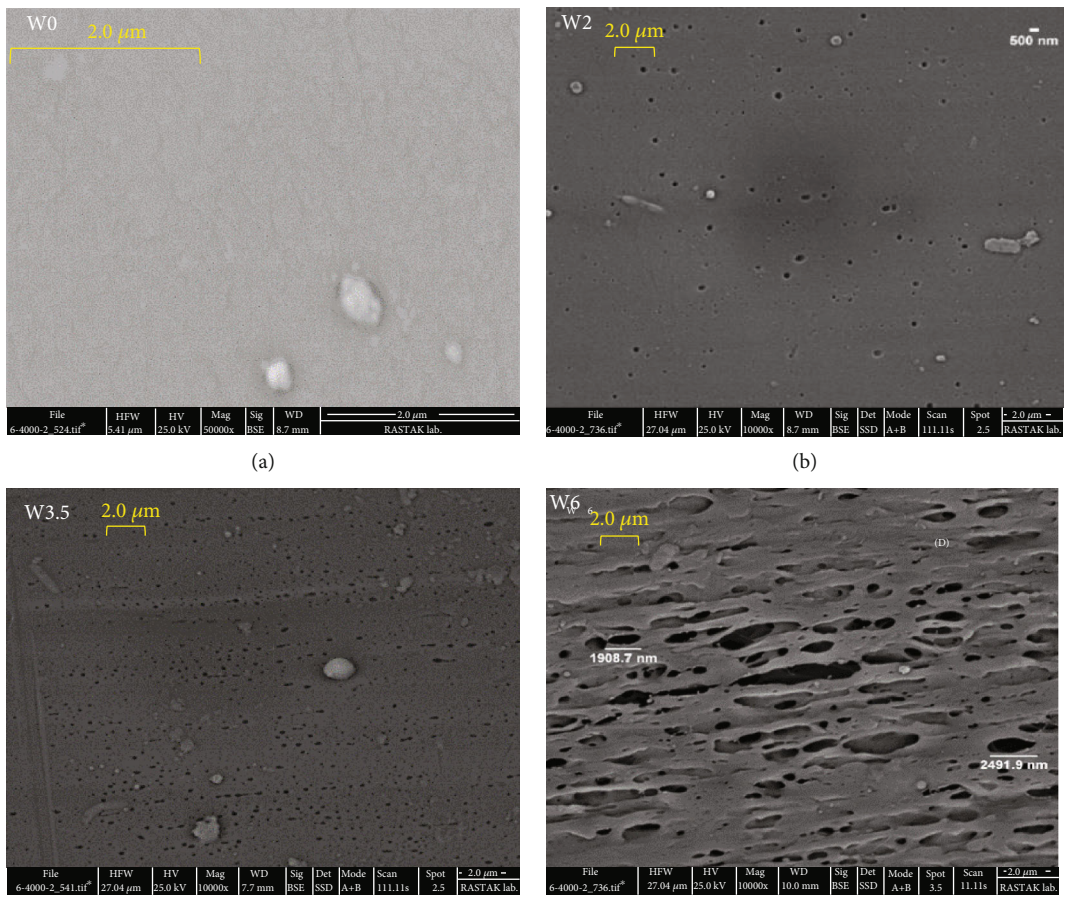

Figure 3: The membrane outer surface morphology of PAN hollow fiber membranes spun from different H_2O concentration: (a) 0 wt%; (b) 2 wt%; (c) 3.5 wt%; (d) 6 wt%.

through a dead-end filtration module with shell-side configuration. To form a lab-scale hollow fiber module, a bundle of 5 dried hollow fiber membranes with 6 cm length each was placed in a hollow metal ring joint, and considering the sealing, the inside of the metal joint was glued with epoxy resin. In contrast, the bottom end of the bundle was open to separate the permeate and retentate parts. The top end of the pile of hollow fibers was potted in epoxy resin. The sealed module with solidified epoxy resin after 24 hours was assembled into a polypropylene tube with a length of 20 cm.

For primary measurement of pure water flux, the membranes were conditioned by flowing deionized water through the shell side of the fibers using a diaphragm pump (JT, Taiwan) for 1 hour under the pressure of 0.8 bar and at a temperature of 23°C so that the system reaches to steady-state condition. The volume of permeate water

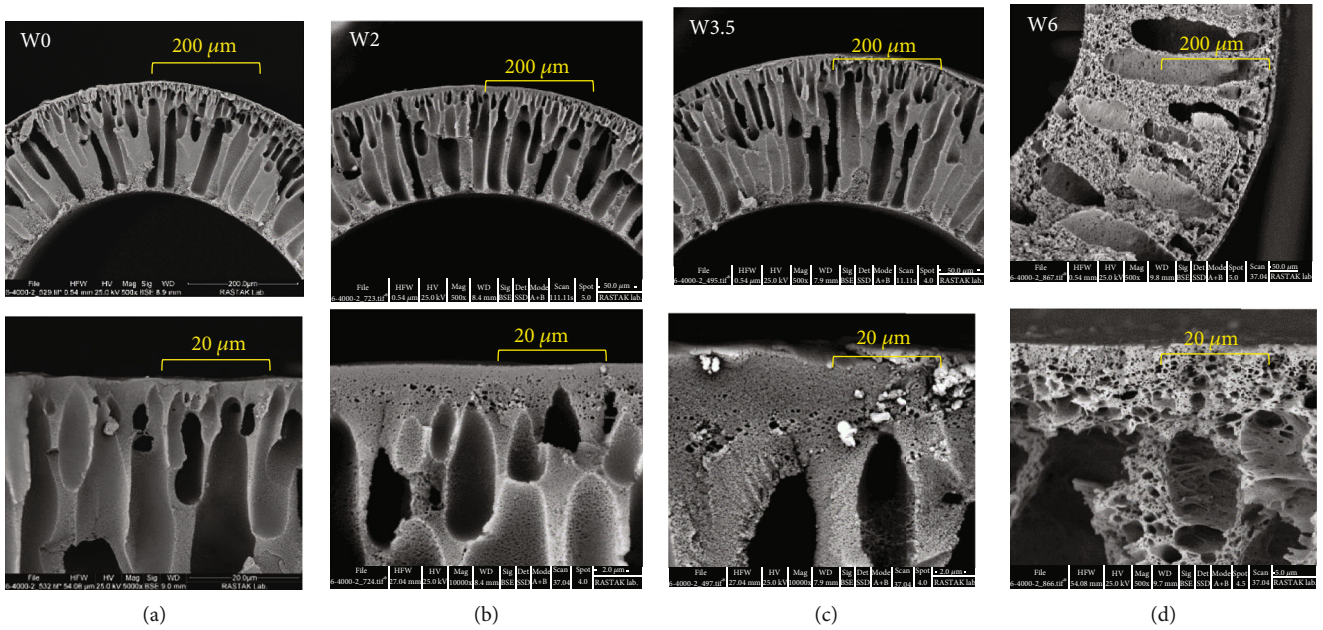

FIGURE 4: Cross-sectional images of PAN hollow fiber membranes spun from different H_2O concentration: (a) 0 wt%; (b) 2 wt%; (c) 3.5 wt%; (d) 6 wt%.

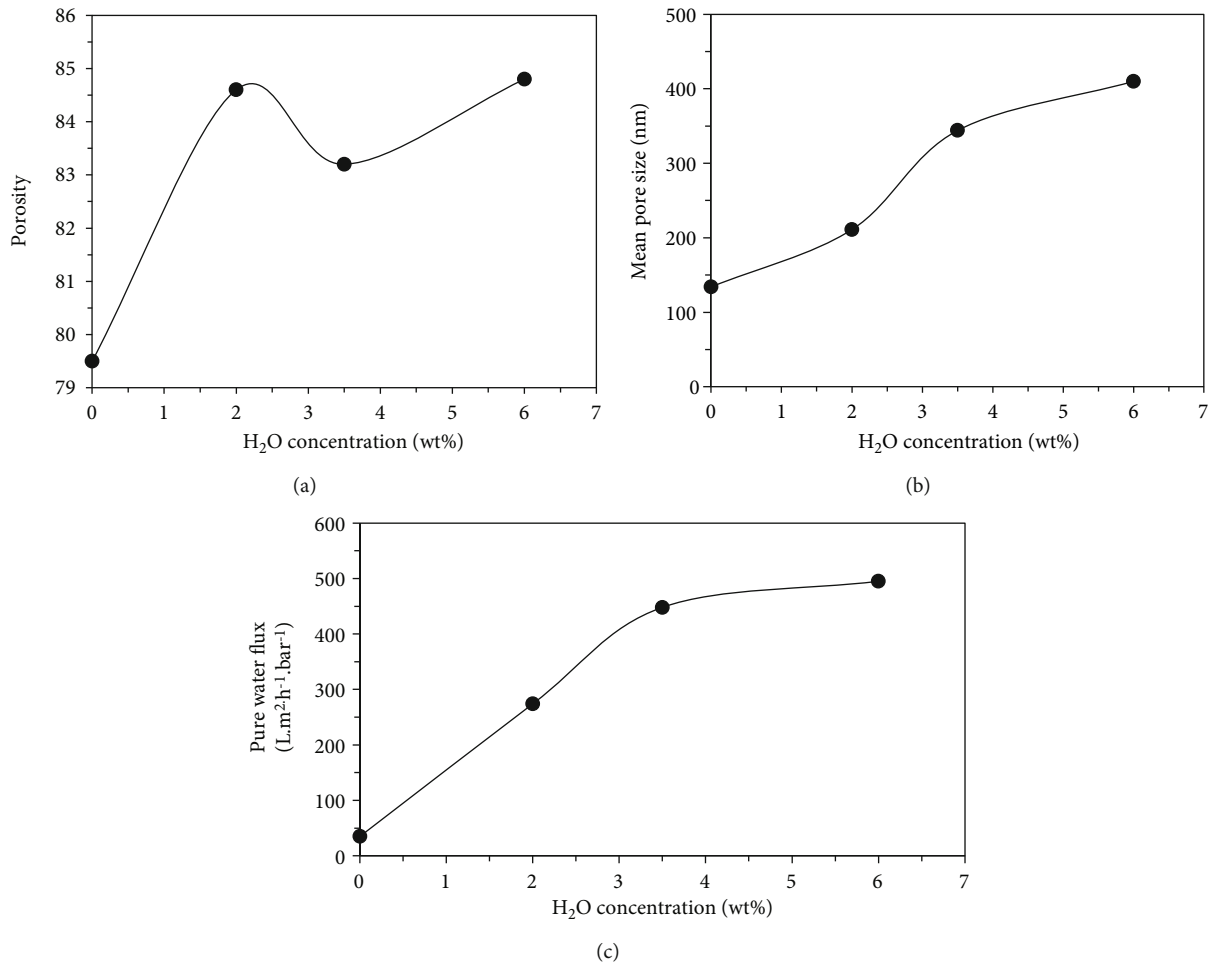

FIGURE 5: Effect of H_2O nonsolvent concentration on the membrane porosity (a), mean pore size (b), and pure water flux (c) of PAN hollow fiber membranes.

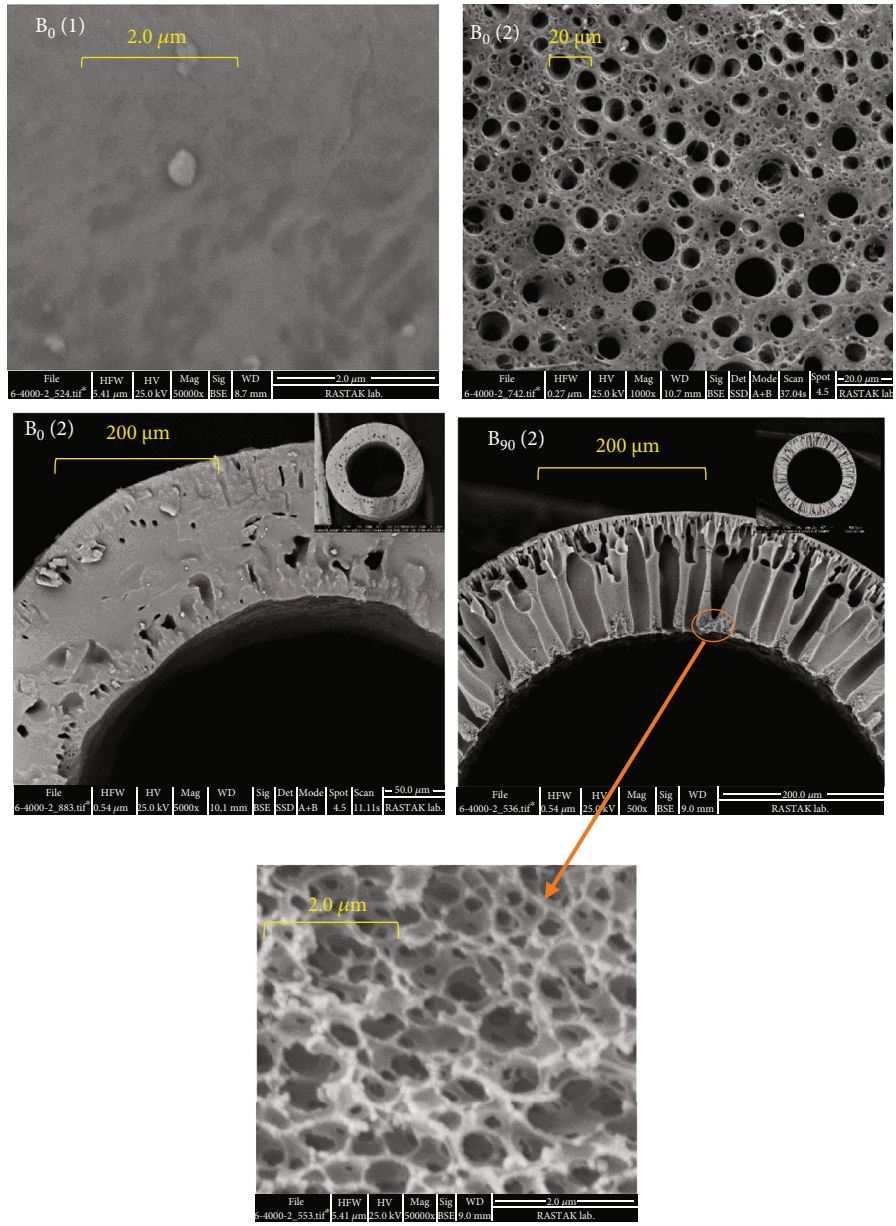

FIGURE 6: Effect of bore fluid type on morphologies of PAN hollow fibers: (a) inner surface; (b–d) cross-section (B_0: pure water, B_{90}: NMP/H_2O = 90/10).

was subsequently collected from the lumen side and measured for 20 min to calculate the initial membrane water flux under the pressure of 0.4 bar and the exact temperature of 23°C of the pure water. Schematic diagram of water separation system setup is shown in Figure 2. The measurements were repeated three times for each sample. Membrane pure water flux J_w (Lit.m^{-2}.hr^{-1}.bar^{-1}) was calculated according to the following equation:

$$J_w = \frac{Q_w}{\Delta P.A_s}, \quad (1)$$

where Q_w (Lit hr^{-1}) is the permeate water volumetric flow, ΔP (bar) is the pressure difference between upstream and downstream, and A_s (m^2) is the effective membrane area. $A = N\pi d_0 l$ equation was used to calculate A_s, where N is the number of hollow fibers in the module, d_0 is the outer diameter of hollow fibers, and l is the length of hollow fibers. The effective membrane area was 9 cm^2.

2.3.3. Porosity and Mean Pore Size Measurement. In order to determine the membrane porosity, membranes were first immersed in deionized water at 25°C for 24 hours. After draining off the excess water on the surface of the wet membranes, clean tissue paper was employed to gently adsorb the excess droplets on the surface of the membrane. The water inside the inner tube of the hollow fibers was removed by air blown into them. A digital scale then weighted membranes with the precision of three decimal places (JS, China)

Table 3: The effect of the bore liquid composition on the pure water flux, porosity, mean pore size, and liquid entry pressure.

Membrane code	Pure water flux (L.m^2.h^{-1}.bar^{-1})	Porosity	Mean pore size (nm)	Liquid entry pressure (bar)
B0	2.6	62	31	4
B90	8.1	86.3	54	0.2

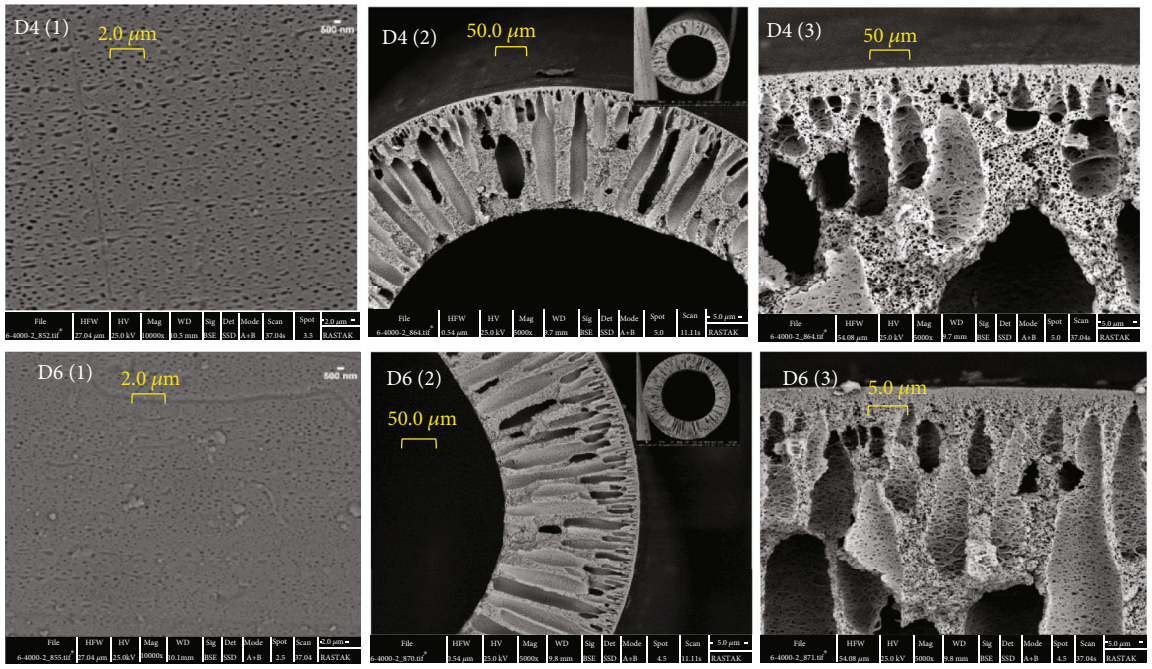

Figure 7: Effect of dope flow rate on morphologies of PAN hollow fibers: (a) cross-section; (b) skin layer cross-section; (c) outer surface (D4: 4 ml/min, D6: 6 ml/min).

Table 4: The effect of the dope flow rate on the pure water flux, porosity, mean pore size, and membrane wall thickness.

Membrane code	Pure water flux (L.m^2.h^{-1}.bar^{-1})	Porosity	Mean pore size (nm)	Membrane wall thickness (μm)
D4	410	84	285	169
D6	472	86.4	331	217

to determine the amount of water in the hollow fiber membrane pores, which were then dried for a total of 24 hours in an oven at 50-60°C, and then, the dry membranes were weighted again. The measurement was repeated three times for each sample. Finally, the membrane porosity was calculated by the following equation [21]:

$$\varepsilon = \frac{W_0 - W_1}{\rho_w . A . b}, \tag{2}$$

where W_0 (gr) is the weight of wet membrane, W_1 (gr) is the weight of dry membrane, ρ_w (gr cm^{-3}) is the density of pure water at room temperature, A (cm^2) is the effective area of membrane sample, and b (cm) is the thickness of the membrane.

Also, to assess mean pore size based on the pure water flux data, Guerout–Elford–Ferry equation was used to determine the average radius of all the pores of the membrane structure; r_m (μm) is calculated from the following equation [22]:

$$r_m = \sqrt{\frac{(2.9 - 1.75\varepsilon) \times 8\eta l Q}{\varepsilon \times A \times \Delta P}}, \tag{3}$$

where ε is membrane porosity, η is water viscosity (8.9×10^{-4} Pa. s), l (m) is membrane thickness (external and internal radius differences), Q (m^{3}s^{-1}) is permeability rate, A (m^2) is the effective area of membrane sample, and ΔP (Pa) is transmembrane pressure.

3. Results and Discussions

3.1. Effect of H_2O as a Nonsolvent Additive. H2O is considered the strongest nonsolvent that a slight addition in the polymer solution has been shown to cause phase instability and decrease the solvent power. Hence, it is possible to bring

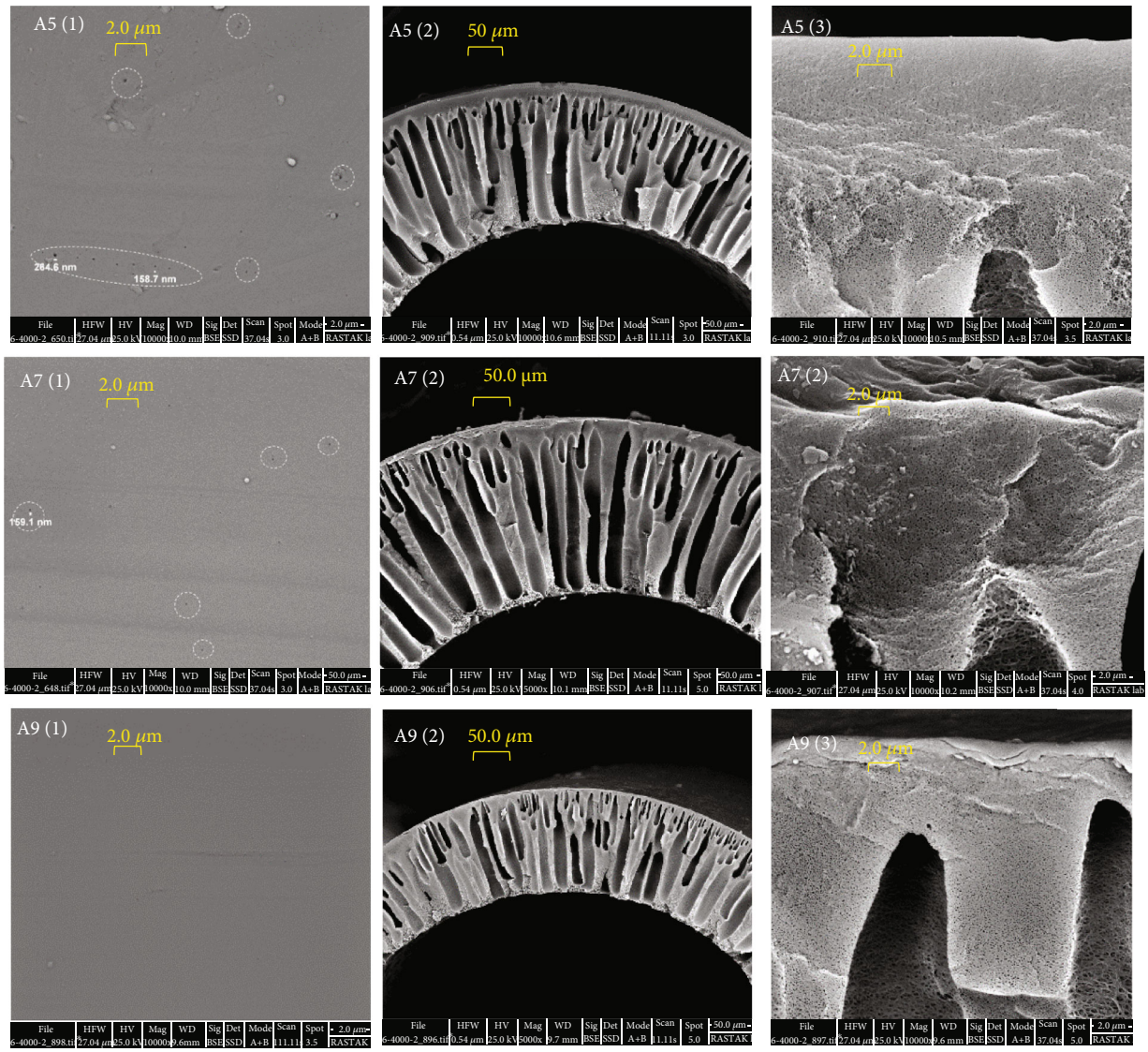

Figure 8: Effect of air gap distance on morphologies of PAN hollow fibers: (a) outer surface; (b) cross-section; (c) skin layer cross-section (A5: 5 cm, A7: 7 cm, A9: 9 cm).

the initial dope composition nearer to the precipitation point without increasing the polymer-polymer interaction; in other words, less solvent is needed to be substituted by the nonsolvent [23]. Here, the effect of H2O concentration as an additive on membrane structure and pure water flux is investigated.

Figures 3 and 4 show the morphology of the outer skin layer and cross-section of hollow fiber PAN membranes fabricated from different water concentrations (0, 2, 3.5, and 6 wt.%). Comparing SEM pictures of fibers W2, W3.5, and W6 with fiber W0 indicates that two visible alterations are noticeable via water addition to the polymer solution. One eliminates the outer close skin layer so that visible pores appear on the surface; the other is the considerable increment of cross-sectional pore size and porosity. As reported in the literature, an ultrathin selective layer and sublayer with large finger-like macrovoids is usually formed when phase inversion is fast. In contrast, slow phase inversion forms a more uniform structure [7, 24]. As the water was added to the polymer solution, the solubility parameter difference between solvent and coagulation bath decreased [12, 25]. Strictly speaking, the initial point of the dope composition goes toward the precipitation point, and the affinity between solvent and nonsolvent reduces and eventually causes reduced phase inversion rate, so the microspores are uniformly distributed through the fiber structure.

The alterations observed in SEM pictures can be analyzed from another point of view. The addition of water clouded the solution and partial phase inversion, which induced a so-called pregelation process before coagulation. Zheng et al. [13] stated that pregelation provides enough time for solid-liquid demixing, accounting for high porosity and pore interconnectivity. The porosity and mean pore size values presented in Figures 5(a) and 5(b) indicate a sudden rise due to the nonsolvent additive. Regarding Figures 3 and 4, increasing water concentration enhanced pore density

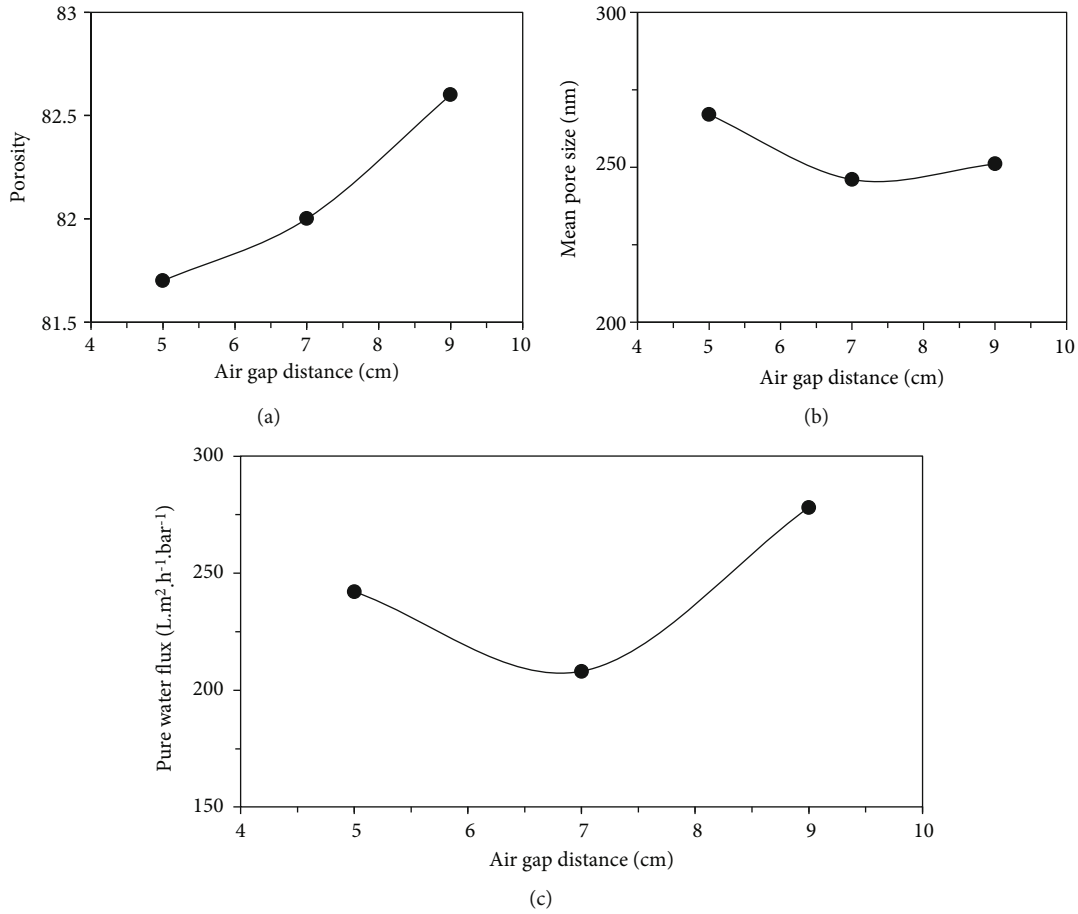

Figure 9: Effect of air gap distance on the membrane porosity (a), mean pore size (b), and pure water flux (c) of PAN hollow fiber membranes.

through the outer surface and cross-section area since the W6 sample represents the most variations. The surface pores of this sample transform from circular shapes to vast voids, and its cross-section morphology displays an asymmetric cellular-like structure.

The effect of H_2O concentration as an additive on pure water flux is shown in Figure 5(c). As can be seen, a nonsolvent additive led to a drastic pure water flux jump of more than ten times. This phenomenon may have originated from eliminating the outer close skin layer and enhancing porosity and pore interconnectivity. Taking the diagram slope into attention reveals that the slope is not proportional to nonsolvent concentration. This observation can be attributed to two opposite effects of increasing nonsolvent concentration. Despite the porosity increment, the polymer solution viscosity increases due to delayed demixing and crystallization. The solution viscosity imposes a resistance to coagulation bath nonsolvent diffusion, which may suppress the macrovoid formation, and finally, the resultant membrane has less facility to water permeation. This trend is according to the porosity and mean pore size values in Figures 5(a) and 5 (b) and cross-section morphology of sample W6 in Figure 4, which includes shorter finger-like macrovoid than other samples.

3.2. Effect of Bore Fluid Type. Two bore fluid solutions containing pure water and a mixture of NMP/H_2O (90/10) were used as internal coagulants and spun fiber structures, and permeation properties were characterized. Figure 6 represents the lumen layer and cross-section morphology of hollow fiber membranes. Bore fluid type has a drastic effect on the morphology. As demonstrated in Figure 6, when solvent-rich solution replaces the bore fluid (water), the rate of phase separation process decreases, which contributes to the elimination of the thin dense surface layer and generation of identical pores and cavities in the membrane structure. It is also apparent from the cross-sectional picture in Figure 6; the rich solvent ratio in bore fluid causes the formation of wall-to-wall finger-like macro-voids through the cross-section.

Table 2 summarizes the effect of bore fluid type on porosity, mean pore size, and pure water flux values. The morphologies describe the considerable increase in porosity and mean pore size in the B90 membrane compared to the B0 sample are represented by the morphologies. The compact structure of fiber B0 can be governed by rapid coagulation of both the inner and outer layers. Rapid inner layer solidification also can be responsible for larger wall thickness that prohibits membrane contraction during air gap.

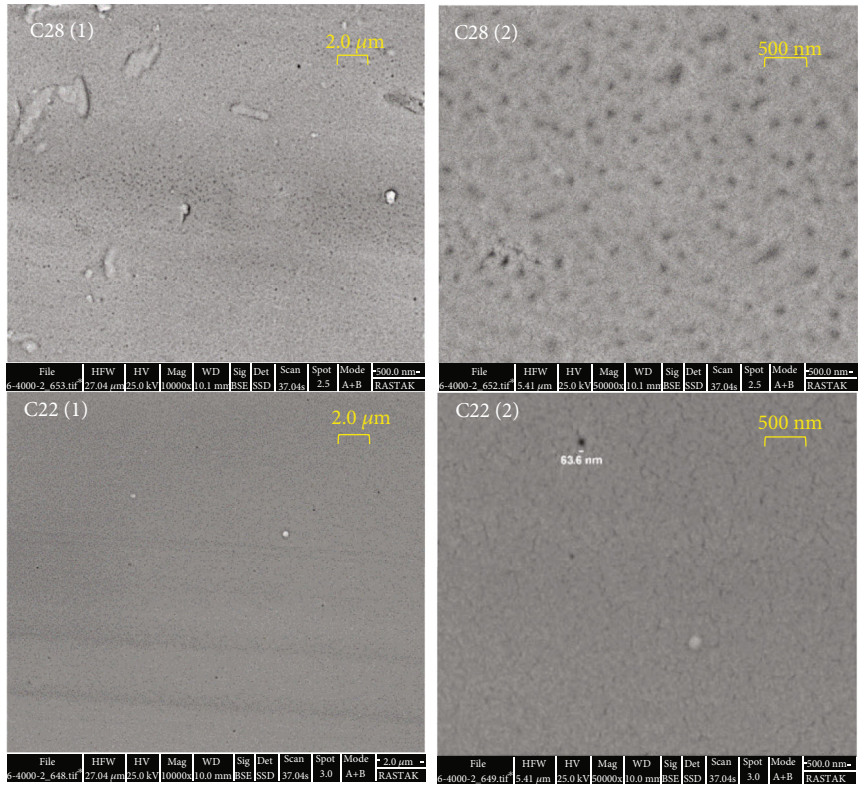

Figure 10: Effect of coagulation bath temperature on outer surface morphologies of PAN hollow fibers: (1) 10000x magnification; (2) 50000x magnification (C22: 22°C, C28: 28°C).

According to Table 3, removing the compact layer enhances the flux of pure water and reduces the permeation entry pressure from 4 to 0.2 bar. These flux variations can be originated from the finger-like and inner skinless morphology of the B90 membrane.

3.3. Effect of Dope Flow Rate. In order to understand the effect of shear rate induced by spinneret wall on the membrane performance, the morphology and structure of microporous membranes under two dope flow rate conditions were investigated. The microscope observed the outer surface, and cross-sections of membranes spun at dope flow rates 4 and 6 ml/min (D4 and D6) were observed by the microscope, as shown in Figure 7.

As can be seen on surface figures, it can be observed that outer surface pores are relatively smaller at higher dope flow rates. Also, careful consideration of the outer selective layer illustrates the thicker outer skin layer formation at a higher dope flow rate. Various studies stated that the shear rate induced by the spinneret annular wall on viscous polymeric solution regulates the lamellar planes and orients of molecular chains. Therefore, shear rate mainly affects the outer surface, and consequently, a more compact and thick outer layer is formed [5, 7, 26].

As shown in Figure 7 and based on porosity and dimension values in Table 4, when the dope flow rate was increased to 6 ml/min, the porosity, fiber outer diameter, mean pore size, and wall thickness all went through a rising trend. This trend can be attributed to expansion and merging cross-sectional cavities and pores, which may be responsible for flux improvement at a higher dope flow rate. These results are in fair agreement with those reported by Shi et al. [27].

Table 5: The effect of the coagulation bath temperature on the pure water flux, porosity, and mean pore size of PAN hollow fiber membrane (C22: 22°C, C28: 28°C).

Membrane code	Pure water flux ($L.m^2.h^{-1}.bar^{-1}$)	Porosity	Mean pore size (nm)
C22	208	82	246
C28	362	86	309

3.4. Effect of Air Gap Distance. Various factors influence hollow fiber membrane structure when fiber passes through the spinneret outlet into the coagulation bath level. In this study, three levels of air gap distance have been used to provide helpful information about the impressibility of hollow fiber membrane by this spinning condition. Figure 8 represents the outer surface and layer and cross-section morphology of hollow fiber membranes spun at air gap distances of 5, 7, and 9 cm, respectively.

Outer surface SEM pictures indicate that the number of visible skin pores under a magnification of 50,000x has decreased by rising air gap distance and finally disappeared at 9 cm. Pore size decrease may be attributed to two reasons; the first caused by external stresses (work) during air gap

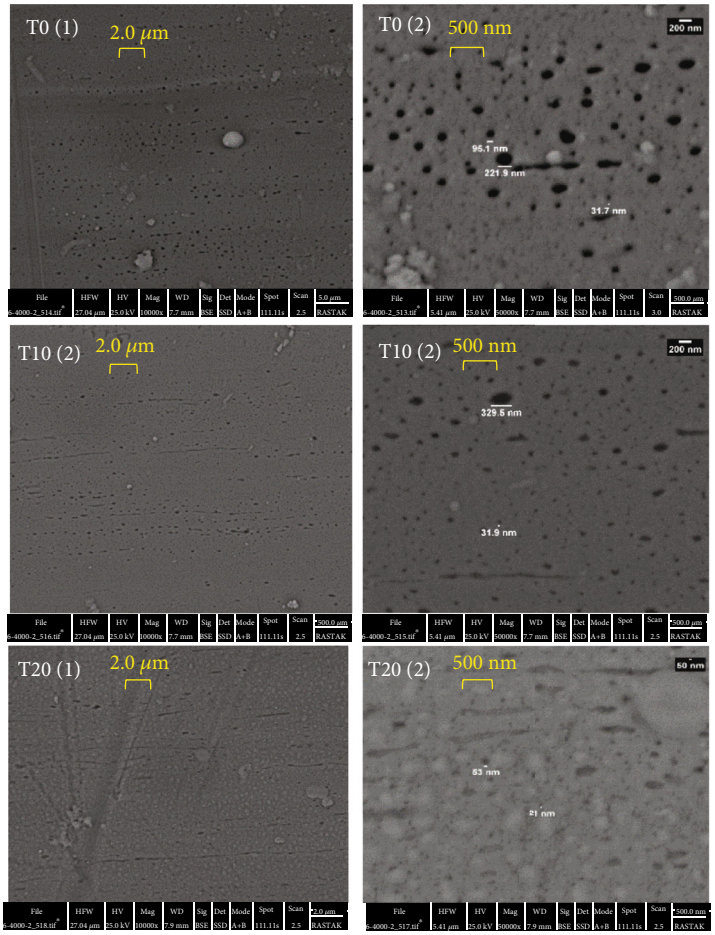

FIGURE 11: Effect of take-up speed on outer surface morphologies of PAN hollow fibers: (a) 10000x magnification; (b) 50000x magnification (T0: free fall; T10: 10% stretch; T20: 20% stretch).

distance is the molecular chain orientation [28]. Molecular chain orientation results in an oriented structure with high packing density through the skin layer; the second is the high affinity of NMP solvent to air humidity that induces partial phase inversion and viscosity increase, enhancing the chance of pore size growth. Cross-sectional pictures show that the most impressibility of air gap rising occurred on the structure near the outer selective layer. It seems that needle-like macrovoids underneath the outer skin of the membranes have grown. This phenomenon could be originated from increasing the contact time of the bore fluid to nascent fiber, which leads to macrovoid size growth as reported by Korminouri et al. [29] and corresponds to porosity uptrend in Figure 8(a).

Figures 9(b) and 9(c) demonstrate mean pore size measurement and pure water flux results, respectively. Firstly, both of them are decreased and then increased by raising the air gap distance, which should be the consequence of opposite variation trends of porosity, skin layer thickness, and surface pore size. An increase in air gap distance entailed porosity uptrend and selective layer and membrane wall thickness which are incremental flux factors. However, the outer selective layer packing density improves, decreasing flux factor. Therefore, domination of mentioned factors could lead to the resultant trend of pure water flux.

3.5. Effect of Coagulation Bath Temperature (CBT). During the hollow fiber membrane spinning process, solidification and membrane formation are completed at the coagulation bath, in which temperature plays a crucial role in the coagulation rate. This study investigated the effect of two different levels of CBT (28 C and 22 C) on membrane structure.

Figure 10 illustrates the impact of CBT on outer surface morphology and pore size. Cooling the bath temperature by 6 degrees leads to a significant decrease in visible surface pores. This alteration can be justified from two points of view. Increasing temperature accelerates mutual diffusivities between the coagulant and the solvent (NMP) in the coagulation bath during phase separation, and nuclei of the polymer-lean phase grow at a higher rate [30]. This may result in a larger outer surface pore size. The SEM figures also can justify the aspect of thermodynamic stability. Wongchitphimon et al. [31] showed that raising the coagulation temperature delayed demixing. An ultrathin dense selective layer and sublayer with large finger-like macrovoids is usually formed when phase inversion is fast [7, 24].

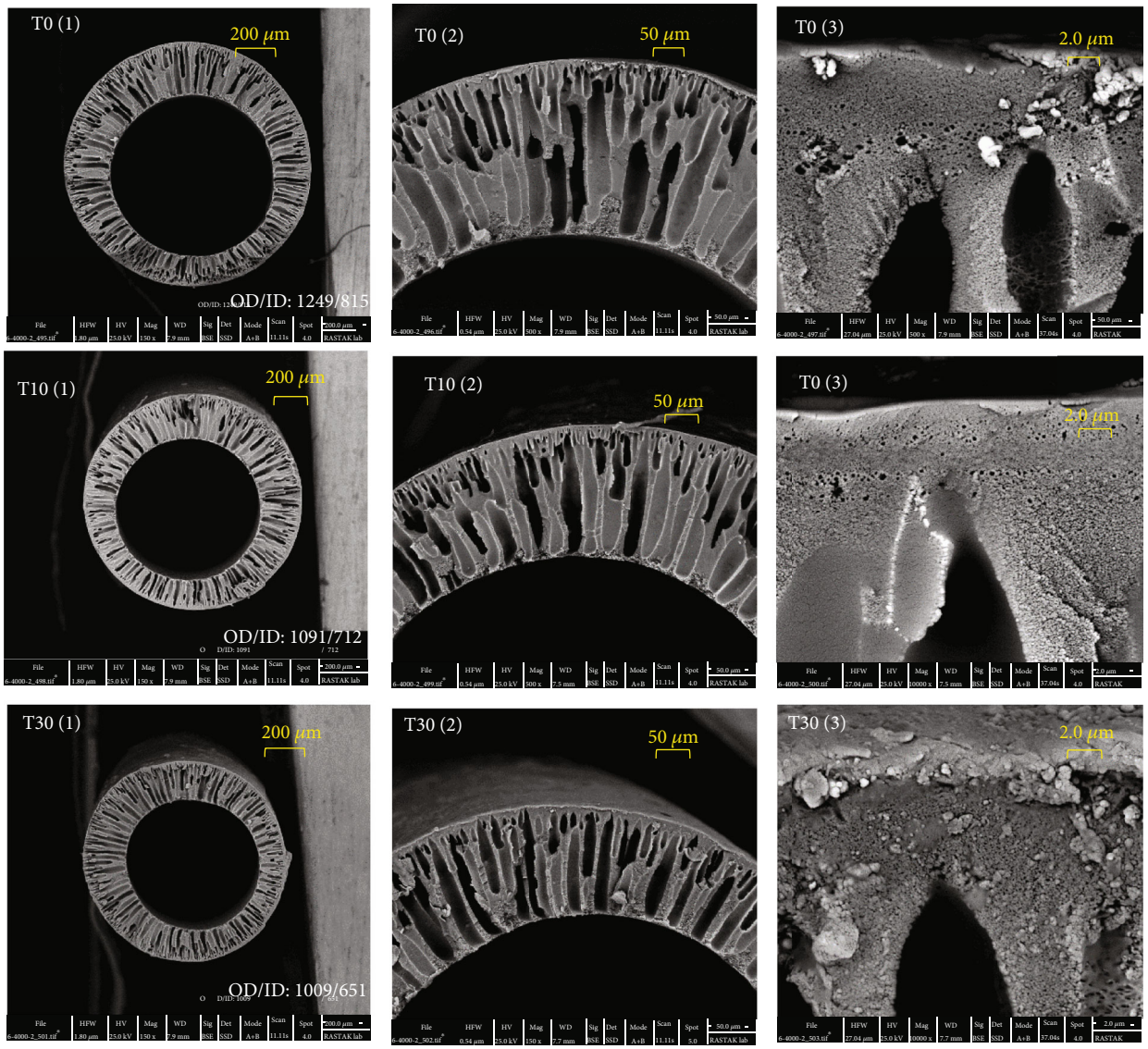

FIGURE 12: Effect of take-up speed on cross sectional morphologies of PAN hollow fibers: (a) 150x magnification; (b) 500x magnification; (c) 10000x magnification (T0: free fall; T10: 10% stretch; T20: 20% stretch).

According to these arguments, it is claimed that warm water is a weaker nonsolvent which leads to a more porous outer surface during a slower precipitation rate.

The pure water flux, porosity, and mean pore size values are listed in Table 5. As was expected, the data decreased at the lower coagulation bath temperature. The pure water flux decrement is most influenced by skin layer formation because it limits membrane permeation. The porosity and mean pore size decrement may result from less nucleus growth and interconnectivity. These results are due to lower mutual diffusivities between the solvent and nonsolvent.

3.6. Effect of Take-Up Speed. The stretch force induced by take-up velocity is a critical spinning condition influencing hollow fiber membrane dimension and performance. In this study, the effect of take-up speed was investigated in the cases of free-falling velocity, 10% stretch, and 20% stretch. The outer surface and cross-section morphology of the membrane are displayed in Figures 11 and 12. Surface pore size became gradually smaller as the take-up speed increased. The cross-sectional SEM pictures illustrate that the more stretch was applied, the fewer micropores in cross-sectional cavities were observed. Moreover, Figure 12 shows that fiber dimensions became smaller at the higher take-up speed; as displayed in Figure 13(d), membrane wall thickness decreased, which means the outer fiber diameter is reduced more rapidly than the inner diameter.

As reported in the literature [27, 32, 33], elongation stretch and the shear stress caused by higher take-up speed are responsible for reducing the outer surface and cross-sectional pore size. On the other hand, stretch force may impose a radial outflow which opposed diffusion of coagulation bath nonsolvent and prohibits pore-forming. Furthermore, high shear stress aligns the PAN macromolecular chains, and thus, a close packing is formed.

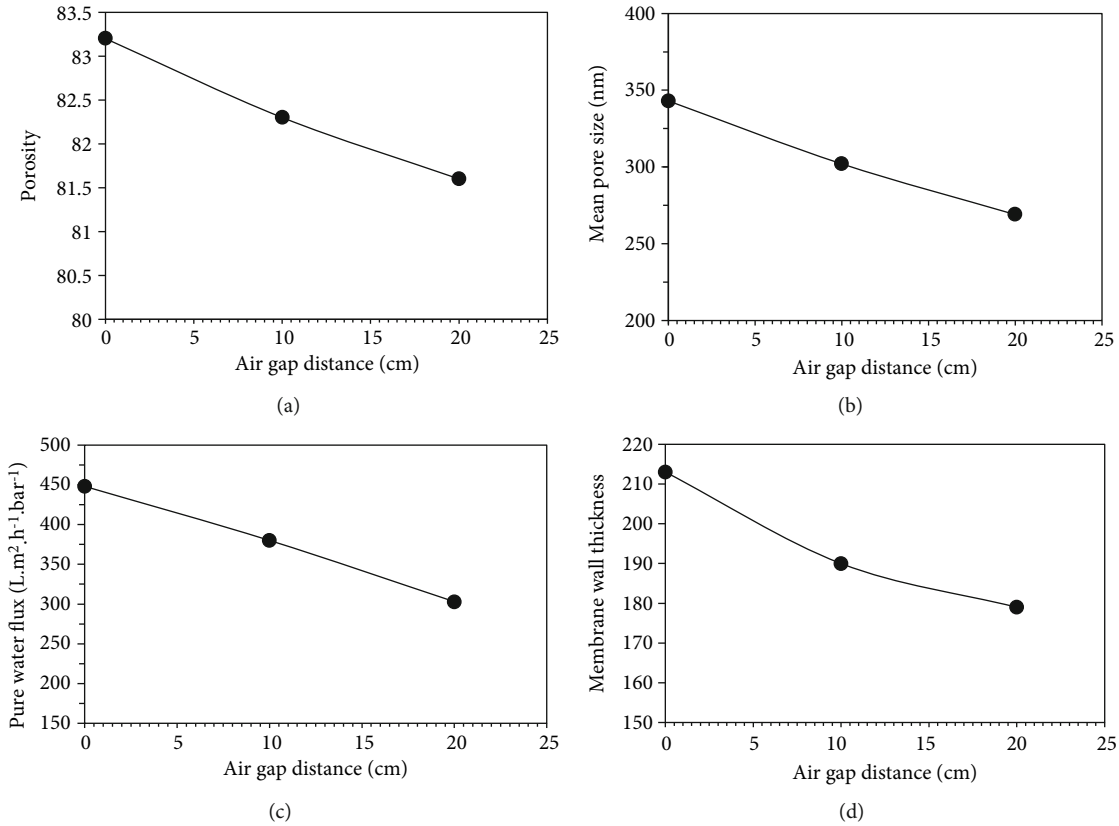

Figure 13: Effect of take-up speed on pure water flux on the membrane porosity (a), mean pore size (b), mean pure size (c), pure water flux (d), and membrane wall thickness.

The effects of take-up speed on pure water flux, mean pore size, porosity, and wall thickness values of the fabricated membrane are shown in Figures 13(a)–13(d), respectively. Noticeably, the shear stress and formation of close packing led to a similar downtrend slope for all parameters with increasing take-up speed. Approximately pure water flux, mean pore size, wall thickness, and porosity decreased by 17%, 12%, 8%, and 1%, respectively, when the take-up speed increased by/to 10%.

4. Conclusion

Hollow fiber membranes were successfully designed and fabricated by a dry/wet-spinning process based on polyacrylonitrile hydrophilic polymer. The morphology and water flux performance of PAN HF membranes were investigated by studying the effects of several design and fabrication parameters to obtain membranes with smaller pore sizes and reasonable water flux. The results revealed that the addition of water as a nonsolvent additive at concentrations of 2 to 6 wt.% into the dope solution significantly affected the membrane morphology and performance. Also, this addition increased the membrane flux up to 17 times and porosity and pore size due to the elimination of the outer dense skin layer and the formation of pores on the outer surface due to delayed demixing phase inversion. The utilization of bore solution with 90 wt.% solvents instead of pure water significantly decreases the permeability threshold pressure of membranes. Also, the removal of the inner skin layer and the sponge-like substructure with micron-scale pores near the inner layer, which is formed through delayed phase inversion, increased cross-sectional porosity. Increasing the dope solution flow rate showed an increment in water flux of the membranes because of the cross-sectional pores. On the other hand, pore size decreased, and the outer selective layer got thicker due to the shear rate applied on the outer surface.

Results showed that due to external stress and partial phase inversion, increasing air gap length allowed the membrane flux and pore size on the outer surface to decrease. However, reducing the coagulation bath temperature by 6°C had a noticeable impact on decreasing surface porosity and pore size. The desired permeability by the design and fabrication parameter adjustment indicated that the PAN HF membranes have promising application in water-based separation processes.

Data Availability

The experiment results and data that support the findings of this study are available from the corresponding author, Mohammad Ali Ghadiri, upon reasonable request.

Conflicts of Interest

The authors declare that they have no conflicts of interest.

References

[1] X. G. Zhang, J. Li, and Z. L. Miao, "Effect of spinning conditions on the morphology of polyacrylonitrile hollow fiber membranes," *Advanced Materials Research*, vol. 221, pp. 146–151, 2011.

[2] A. El-Hadidy, *Removal of Enteric Viruses by Ultrafiltration Membranes*, UWSpace, 2011.

[3] A. Antony, J. Blackbeard, and G. Leslie, "Removal efficiency and integrity monitoring techniques for virus removal by membrane processes," *Critical Reviews in Environmental Science and Technology*, vol. 42, no. 9, pp. 891–933, 2012.

[4] S. Kobayashi and K. Müllen, *Encyclopedia of Polymeric Nanomaterials-with 2021 Figures and 146 Tables*, Springer, 2015.

[5] C. Y. Feng, K. C. Khulbe, T. Matsuura, and A. F. Ismail, "Recent progresses in polymeric hollow fiber membrane preparation, characterization and applications," *Separation and Purification Technology*, vol. 111, pp. 43–71, 2013.

[6] F. Liu, N. A. Hashim, Y. Liu, M. R. M. Abed, and K. Li, "Progress in the production and modification of PVDF membranes," *Journal of Membrane Science*, vol. 375, no. 1-2, pp. 1–27, 2011.

[7] N. Peng, N. Widjojo, P. Sukitpaneenit et al., "Evolution of polymeric hollow fibers as sustainable technologies: past, present, and future," *Progress in Polymer Science*, vol. 37, pp. 1401–1424, 2012.

[8] A. Venault, Y. Chang, D.-M. Wang, and D. Bouyer, "A review on polymeric membranes and hydrogels prepared by vapor-induced phase separation process," *Polymer Reviews*, vol. 53, no. 4, pp. 568–626, 2013.

[9] V. Laninovic, "Relationship between type of nonsolvent additive and properties of polyethersulfone membranes," *Desalination*, vol. 186, no. 1-3, pp. 39–46, 2005.

[10] A. Mansourizadeh and A. F. Ismail, "Preparation and characterization of porous PVDF hollow fiber membranes for CO2 absorption: effect of different non-solvent additives in the polymer dope," *International Journal of Greenhouse Gas Control*, vol. 5, no. 4, pp. 640–648, 2011.

[11] Z.-G. Wang, Z.-K. Xu, and L.-S. Wan, "Modulation the morphologies and performance of polyacrylonitrile-based asymmetric membranes containing reactive groups: effect of non-solvents in the dope solution," *Journal of Membrane Science*, vol. 278, no. 1-2, pp. 447–456, 2006.

[12] Z.-L. Xu and F. Alsalhy Qusay, "Polyethersulfone (PES) hollow fiber ultrafiltration membranes prepared by PES/non-solvent/NMP solution," *Journal of Membrane Science*, vol. 233, no. 1-2, pp. 101–111, 2004.

[13] L. Zheng, Z. Wu, Y. Zhang, Y. Wei, and J. Wang, "Effect of non-solvent additives on the morphology, pore structure, and direct contact membrane distillation performance of PVDF-CTFE hydrophobic membranes," *Journal of Environmental Sciences*, vol. 45, pp. 28–39, 2016.

[14] B. Chakrabarty, A. K. Ghoshal, and M. K. Purkait, "Preparation, characterization and performance studies of polysulfone membranes using PVP as an additive," *Journal of Membrane Science*, vol. 315, no. 1-2, pp. 36–47, 2008.

[15] Y. Liu, G. H. Koops, and H. Strathmann, "Characterization of morphology controlled polyethersulfone hollow fiber membranes by the addition of polyethylene glycol to the dope and bore liquid solution," *Journal of Membrane Science*, vol. 223, no. 1-2, pp. 187–199, 2003.

[16] C. H. Loh, R. Wang, L. Shi, and A. G. Fane, "Fabrication of high performance polyethersulfone UF hollow fiber membranes using amphiphilic Pluronic block copolymers as pore-forming additives," *Journal of Membrane Science*, vol. 380, no. 1-2, pp. 114–123, 2011.

[17] J.-J. Qin, Y.-M. Cao, Y.-Q. Li, Y. Li, M.-H. Oo, and H. Lee, "Hollow fiber ultrafiltration membranes made from blends of PAN and PVP," *Separation and Purification Technology*, vol. 36, no. 2, pp. 149–155, 2004.

[18] A. Razmjou, A. Resosudarmo, R. L. Holmes, H. Li, J. Mansouri, and V. Chen, "The effect of modified TiO_2 nanoparticles on the polyethersulfone ultrafiltration hollow fiber membranes," *Desalination*, vol. 287, pp. 271–280, 2012.

[19] N. A. Hamid, A. F. Ismail, T. Matsuura et al., "Morphological and separation performance study of polysulfone/titanium dioxide (PSF/TiO_2) ultrafiltration membranes for humic acid removal," *Desalination*, vol. 273, no. 1, pp. 85–92, 2011.

[20] D. Wang, K. Li, and W. K. Teo, "Porous PVDF asymmetric hollow fiber membranes prepared with the use of small molecular additives," *Journal of Membrane Science*, vol. 178, no. 1-2, pp. 13–23, 2000.

[21] A. Salahi, T. Mohammadi, R. M. Behbahani, and M. Hemati, "PES and PES/PAN blend ultrafiltration hollow fiber membranes for oily wastewater treatment: preparation, experimental investigation, fouling, and modeling," *Advances in Polymer Technology*, vol. 34, no. 3, 2015.

[22] E. Saljoughi, M. Amirilargani, and T. Mohammadi, "Effect of poly(vinyl pyrrolidone) concentration and coagulation bath temperature on the morphology, permeability, and thermal stability of asymmetric cellulose acetate membranes," *Journal of Applied Polymer Science*, vol. 111, no. 5, pp. 2537–2544, 2011.

[23] L. Shi, R. Wang, Y. Cao, D. T. Liang, and J. H. Tay, "Effect of additives on the fabrication of poly(vinylidene fluoride-co-hexafluropropylene) (PVDF-HFP) asymmetric microporous hollow fiber membranes," *Journal of Membrane Science*, vol. 315, no. 1-2, pp. 195–204, 2008.

[24] W. J. Koros, "Synthetic polymeric membranes: a structural perspective, second edition by R. E. Kesting, John Wiley & Sons, 1985, 348 pp," *AICHE Journal*, vol. 33, no. 1, pp. 171-172, 1987.

[25] C. Hansen, *Hansen Solubility Parameters: A User's Handbook*, Elsevier, 2nd edition, 2012.

[26] T.-S. Chung, J.-J. Qin, A. Huan, and K.-C. Toh, "Visualization of the effect of die shear rate on the outer surface morphology of ultrafiltration membranes by AFM," *Journal of Membrane Science*, vol. 196, no. 2, pp. 251–266, 2002.

[27] L. Shi, R. Wang, and Y. Cao, "Effect of the rheology of poly (vinylidene fluoride-co-hexafluropropylene) (PVDF–HFP) dope solutions on the formation of microporous hollow fibers used as membrane contactors," *Journal of Membrane Science*, vol. 344, no. 1-2, pp. 112–122, 2009.

[28] T.-S. Chung, "The limitations of using Flory-Huggins equation for the states of solutions during asymmetric hollow-fiber formation," *Journal of Membrane Science*, vol. 126, no. 1, pp. 19–34, 1997.

[29] F. Korminouri, M. Rahbari-Sisakht, D. Rana, T. Matsuura, and A. F. Ismail, "Study on the effect of air-gap length on properties and performance of surface modified PVDF hollow fiber membrane contactor for carbon dioxide absorption," *Separation and Purification Technology*, vol. 132, pp. 601–609, 2014.

[30] M. Amirilargani, E. Saljoughi, T. Mohammadi, and M. R. Moghbeli, "Effects of coagulation bath temperature and polyvinylpyrrolidone content on flat sheet asymmetric polyethersulfone membranes," *Polymer Engineering and Science*, vol. 50, no. 5, pp. 885–893, 2010.

[31] S. Wongchitphimon, R. Wang, R. Jiraratananon, L. Shi, and C. H. Loh, "Effect of polyethylene glycol (PEG) as an additive on the fabrication of polyvinylidene fluoride-co-hexafluropropylene (PVDF-HFP) asymmetric microporous hollow fiber membranes," *Journal of Membrane Science*, vol. 369, no. 1-2, pp. 329–338, 2011.

[32] D. Li, T.-S. Chung, and R. Wang, "Morphological aspects and structure control of dual-layer asymmetric hollow fiber membranes formed by a simultaneous co-extrusion approach," *Journal of Membrane Science*, vol. 243, no. 1-2, pp. 155–175, 2004.

[33] P. Sukitpaneenit and T.-S. Chung, "Molecular design of the morphology and pore size of PVDF hollow fiber membranes for ethanol-water separation employing the modified pore-flow concept," *Journal of Membrane Science*, vol. 374, no. 1-2, pp. 67–82, 2011.